PASJ: Publ. Astron. Soc. Japan **50**, 155–162 (1998)

Measurements of the 492 GHz Atmospheric Opacity at Pampa la Bola and Rio Frio in Northern Chile

Tomoya HIROTA, Satoshi YAMAMOTO, and Yutaro SEKIMOTO
Department of Physics and Research Center for the Early Universe, School of Science, The University of Tokyo, Bunkyo-ku, Tokyo 113-0033
E-mail(TH): hirota@taurus.phys.s.u-tokyo.ac.jp
and
Kotaro KOHNO, Naomasa NAKAI, and Ryohei KAWABE
Nobeyama Radio Observatory, Minamimaki-mura, Minamisaku-gun, Nagano 384-1305*

(Received 1997 November 4; accepted 1998 January 13)

Abstract

We have developed a transportable 492 GHz tipping radiometer to measure the atmospheric opacity at potential sites for future ground-based astronomical observations in the submillimeter-wave band. With this radiometer, we measured the atmospheric opacity at two sites in northern Chile, Pampa la Bola (elevation 4800 m) and Rio Frio (elevation 4100 m), each for a few days. The 492 GHz opacity mostly ranged from 0.5 to 1.5 during the measurements. The 220 GHz opacity was also measured at the same time. The 492 GHz opacity correlates well with the 220 GHz opacity, the ratio between the 492 and 220 GHz opacities being 21.2 ± 0.4. This result supports the standard atmospheric model, and can be used to evaluate the observable fraction of time for submillimeter-wave observations on the basis of the long-term 220 GHz opacity data.

Key words: Earth: atmosphere — Instruments — Interferometers

1. Introduction

The large millimeter- and submillimeter-wave array (LMSA) is a future astronomical project planned for the early 21st century (e.g., Ishiguro 1997). The array will consist of 50 high-precision antennas, each with a diameter of about 10 m, which will be distributed to the maximum base-line length of about 10 km, and will realize an angular resolution of 0.″1 to 0.″01 in millimeter- and submillimeter-wave observations. The large collecting area and high angular resolution of the array will provide us good opportunities to observe spectral lines and continuum emission from various kinds of new astronomical objects. Particularly, submillimeter-wave observations comprise a key aspect for the LMSA project. There are a number of important spectral lines of fundamental molecules, atoms, and ions in the submillimeter-wave region, and hence, their observations with high spatial resolution would unveil the nature of protoplanetary nebulae, protogalaxies, and other important targets.

Since the submillimeter-wave emission from astronomical objects suffers from strong absorption by water vapor and oxygen molecules contained in the atmosphere, a high-altitude, dry site is essential for sensitive submillimeter-wave observations. On the basis of extensive and systematic studies on a possible site for LMSA by the Nobeyama Radio Observatory (NRO) group (e.g., Kohno et al. 1995), two sites in northern Chile, Rio Frio (elevation 4100 m) and Pampa la Bola (elevation 4800 m), have been found to be good potential candidates. In order to evaluate the observing conditions quantitatively, a long-term measurement of the 220 GHz atmospheric opacity was carried out at the Rio Frio site with an automatic tipping radiometer for about 3 years (Holdaway et al. 1996). Although such a long-term measurement at the Pampa la Bola site has not been carried out so far, the NRAO group is measuring the 225 GHz opacity at the Chajnantor site (elevation 5050 m), which is located about 7 km south west of Pampa la Bola (Holdaway et al. 1996). Since there have been no measurements of the submillimeter-wave opacity at these sites in Chile so far, it was usually estimated from the 225 GHz opacity with the aid of an atmospheric model or an empirical relation. For example, the following empirical relation was found in Mauna Kea, Hawaii on the basis of direct measurements of the 492 GHz opacity (Masson 1994):

$$\tau_{492} = 20\ (\tau_{225} - 0.01), \tag{1}$$

where τ_{492} and τ_{225} represent the opacities at 492 GHz

* Nobeyama Radio Observatory (NRO) is a branch of the National Astronomical Observatory, an inter-university research institute operated by the Ministry of Education, Science, Sports and Culture.

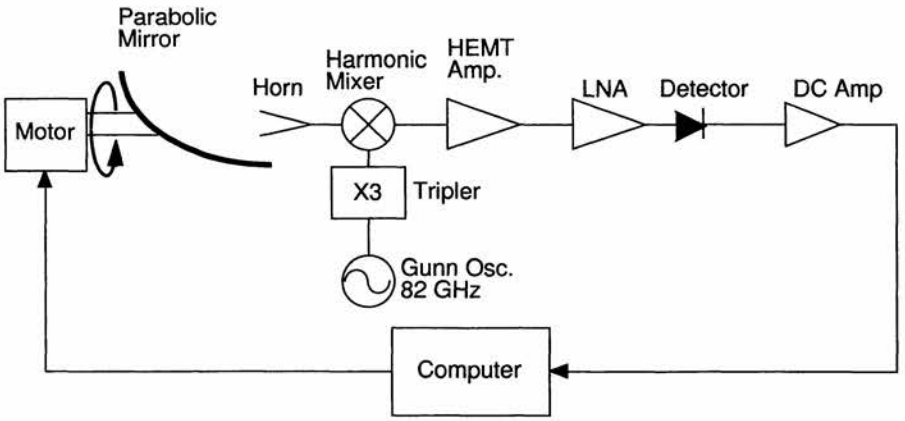

Fig. 1. Block diagram of the transportable 492 GHz radiometer.

and 225 GHz, respectively. The 492 GHz opacity is often regarded as being a representative value of the submillimeter-wave opacity. This is one of the important frequencies in the submillimeter-wave region, since a spectral line of the neutral carbon atom ($^3P_1$–$^3P_0$; 492.160651 GHz) lies at this frequency (Yamamoto, Saito 1991).

So far, equation (1) has been employed at various sites without any further experiments and considerations. Since the distribution of water vapor might depend on the local meteorology to a certain extent, the atmospheric conditions could be different from site to site. Hence, it is of fundamental importance to directly measure the 492 GHz opacity at the two potential sites for LMSA in order to evaluate the observational feasibility in the submillimeter-wave region. On the basis of this motivation, we here report on simultaneous measurements of the 220 GHz and 492 GHz opacities at Pampa la Bola and Rio Frio.

2. Apparatus

We prepared a transportable 492 GHz tipping radiometer for this purpose. A block diagram of the radiometer is shown in figure 1. This is a modified version of the 220 GHz radiometer used at Mt. Fuji for two years (Sekimoto et al. 1996). It has an offset parabolic mirror with an effective aperture of 50 mm, which can rotate around the elevation axis by use of a stepping motor. The beam size (HPBW) at 492 GHz is 1°, and the stepping angle of the motor is 0.°72. A GaAs Schottky-diode harmonic mixer with a conical feed horn is set at the focus of the mirror. The mixer is operated in the double-sideband (DSB) mode at ambient temperature. A local oscillator for the mixer is a combination of a Gunn oscillator and a frequency tripler. This provides us with an output of 493.5 GHz. The Gunn oscillator is operated in a free-run mode. The intermediate frequency (IF) of the mixer is taken to be 1.5 GHz with a bandwidth of about 500 MHz. Thus, a frequency range of 492 ± 0.25 GHz is in the lower side band of the mixer, and that of 495 ± 0.25 GHz is in the upper side band. A low-noise HEMT amplifier was employed for the first-stage IF amplifier, whereas a FET amplifier was used for the second stage. The total output power was detected by a Schottky-diode detector, and its DC output was amplified to about 1 V for an A/D conversion. The system-noise temperature was measured to be 6000 K in the laboratory. However, we operated the mixer with a relatively small power of the local oscillator for a safety reason during the actual observations at the sites. As a result, the system noise was about twice the above value. The thermal noise per integration is 1.2 K when the system noise temperature is 12000 K.

The stepping motor is controlled by an output pulse voltage from a note-book-type computer. First, the mirror is set to a zenith angle of −90° (initial position), where the negative sign of the zenith angle corresponds to the western direction in Pampa la Bola, and the east in Rio Frio; then, a tipping scan ia started. Two hundred and forty steps cover the zenith angle from −90° to 82.°8, and another 240 steps are used for moving back to the initial position. It takes 120 s for the forward and backward scans. The total power is recorded at each step with an integration time of about 0.2 s. The data obtained in the forward and backward scans are averaged in order to compensate for any small drift in the output voltage due to a slow variation in the amplifier gain.

The system can be accommodated in an aluminum carrying case, and is transportable to any site. The total weight of the system, including the case, is about 25 kg,

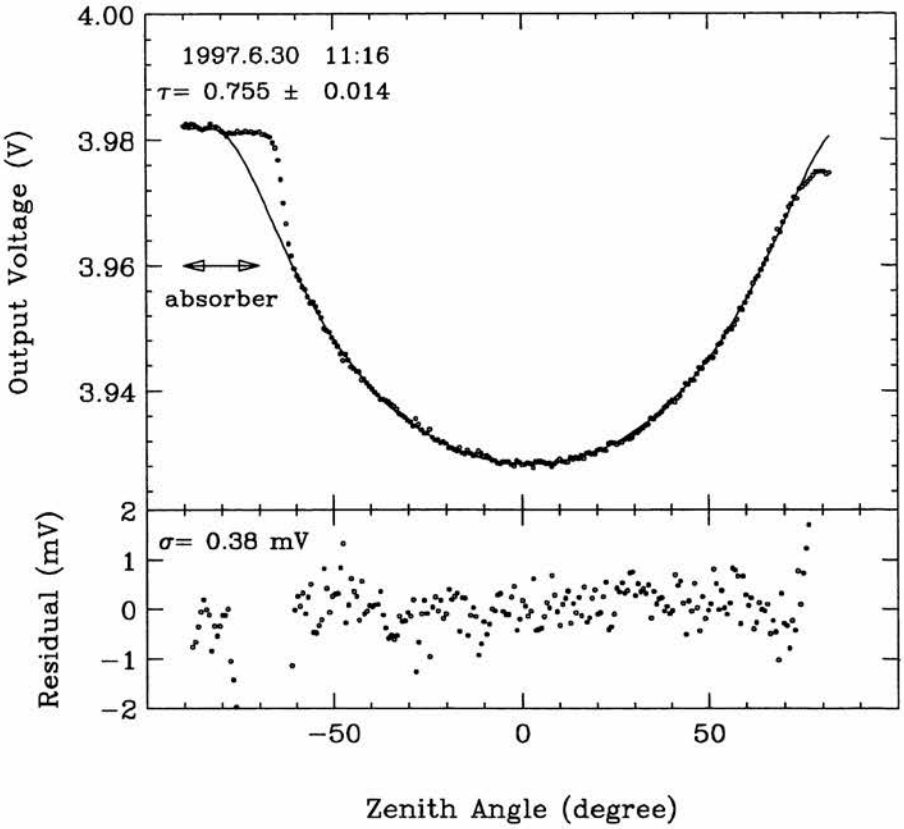

Fig. 2. Example of tipping scan data taken at Pampa la Bola. Data for the zenith angle from −90° to −70° corresponds to the absorber temperature for calibration. Solid line is the best fit line of the equation (2); in which τ_0 is calculated to be 0.755 ± 0.014. The residuals are plotted in the lower figure.

and the total electric power required is about 30 W. If we change the mixer and the parabolic mirror, the system can be used for measurements at 220 GHz.

3. Observations

We measured the 492 GHz atmospheric opacity at Pampa la Bola from 1997 June 28 to July 1. We set the 492 GHz radiometer at the south of a container house. In this case, the container worked as a sun shade for our radiometer, and we were able to avoid any heating effect on the radiometer due to solar radiation. Tipping scans were carried out along the west-to-east direction. The 220 GHz transportable radiometer (Kohno et al. 1995) was also set beside the 492 GHz radiometer, and tipping scans were made toward nearly the same direction of the sky.

At Pampa la Bola, we mainly used electricity supplied from solar panels and backup batteries. Because of the limited capability of electricity, we also used a generator, particularly for night observations. The observations were carried out in an automatic way. Although the 492 GHz opacity was usually measured every 10 min, data were sometimes taken every 2 min in order to study any short-time variation in the opacity. On the other hand, the 220 GHz opacity was measured every 1 min. Finally, we measured the 492 GHz opacity for about 40 hr out of 96 hr of our observing run at Pampa la Bola. The weather was almost fine during the observations. A typical result for a tipping scan by the 492 GHz radiometer is shown in figure 2.

The 492 GHz opacity at Rio Frio was measured from 1997 July 2 to 4. As in the case at Pampa la Bola, the 492 GHz radiometer was set at the south side of the container house, and the tipping scans were carried out toward a east-to-west direction. At Rio Frio, we used electricity supplied from solar panels and backup batteries. The 492 GHz opacity was measured every 10 min in an automatic way. The opacity was measured for 40 hr in total at Rio Frio. The 220 GHz opacity toward the same direction was measured every 1 min by a radiometer placed at the container house. The weather was fine in July 2, but we experienced a thin cloud in July 4.

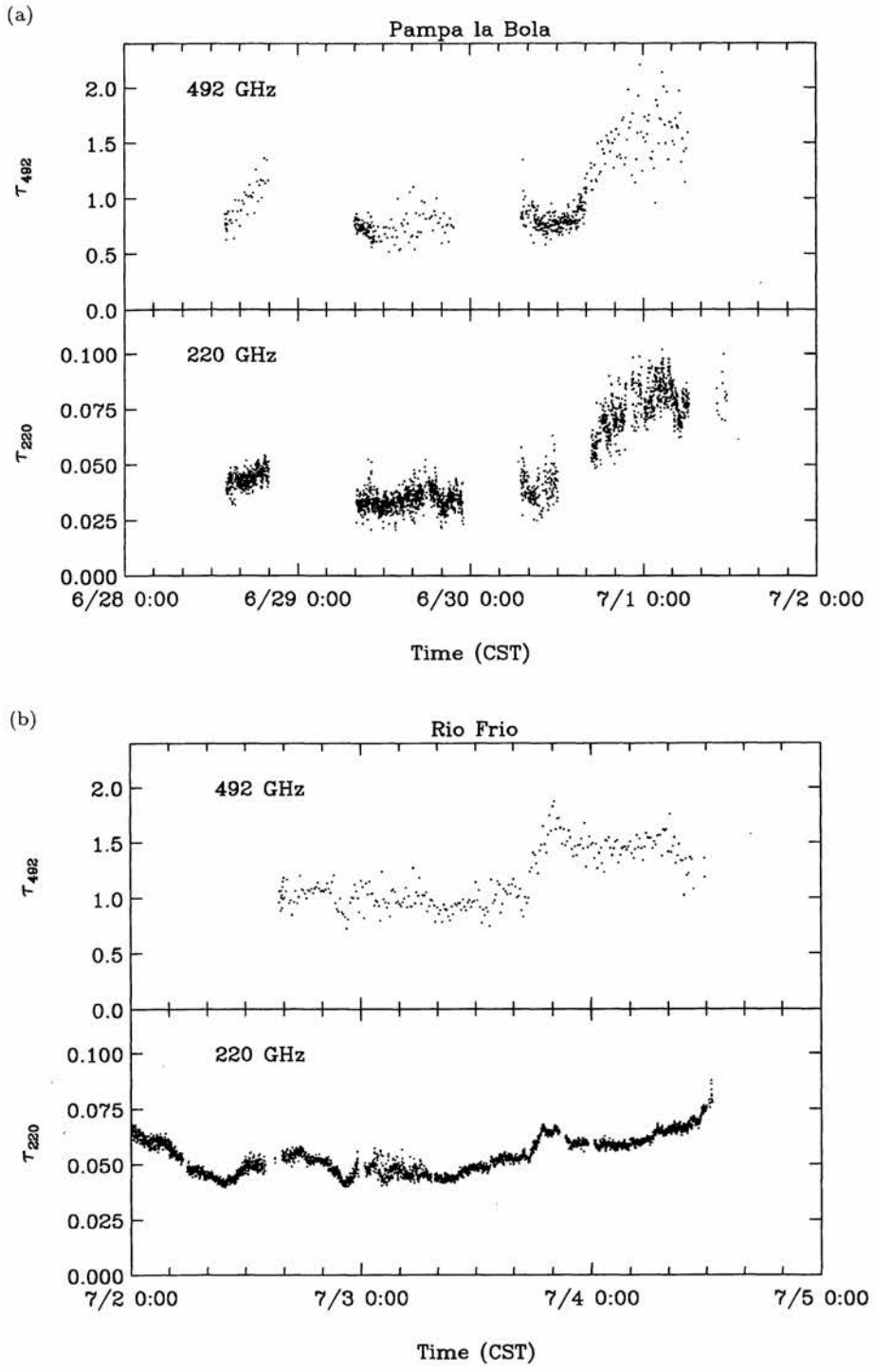

Fig. 3. Time variation of the 492 GHz and 220 GHz opacities measured simultaneously at Pampa la Bola (a) and Rio Frio (b). The time is Chilean standard time (CST).

4. Analysis

Based on the observed tipping data, we evaluated the 492 GHz opacity toward the zenith direction τ_0 by a least-squares method. We assumed a plane-parallel structure of the atmosphere, and used the following equation to fit the data:

$$V_{\rm obs}(z) = V_{\rm sky}[1 - \exp(-\tau_0 \sec z)] + V_{\rm sys}, \quad (2)$$

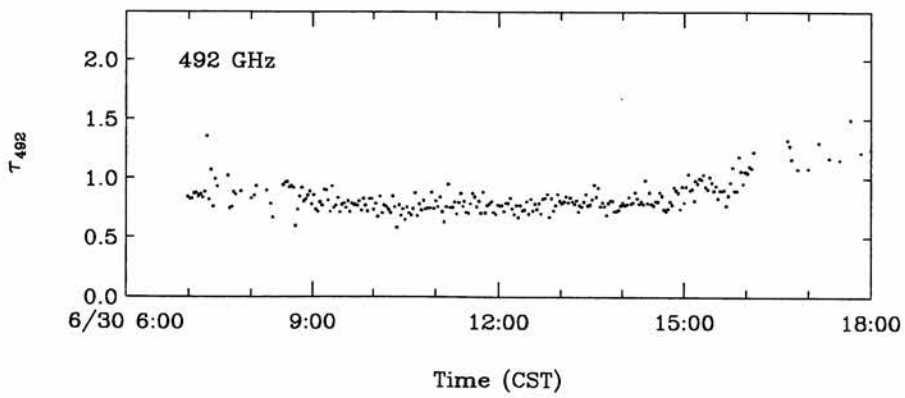

Fig. 4. Short-period variation of the opacity of 492 GHz observed on 1997 June 30 at Pampa la Bola.

where $V_{\rm obs}$ represents the observed output voltage for a zenith angle of z, $V_{\rm sky}$ the voltage corresponding to the atmospheric temperature, and $V_{\rm sys}$ the voltage caused by system noise. We also employed the following constraint in the fit:

$$V_{\rm abs} = V_0 + V_{\rm sys}, \tag{3}$$

where $V_{\rm abs}$ stands for the output voltage when the mirror looks at the absorber and V_0 the voltage caused by the absorber. We assumed that the absorber temperature was the same as the ambient temperature (i.e., $V_0 = V_{\rm sky}$).

We carried out a non-linear least-squares fit using the Gauss-Newton method in order to determine the zenith opacity. Since the opacity at 492 GHz is quite high, the data at a larger zenith angle suffer very much from an error of the zenith angle, which was estimated to be about 2°. We thus used the data for the zenith angle from −36° to 36° in the fit. All of the data within this range of the zenith angle were equally weighted. For most cases, the fit was fairly good, even outside the above range, i.e., typically for the zenith angle from −60° to 60°. An example of the fit is shown in figure 2.

The temperature of the sky may be different from that of the absorber. In this case, the temperature difference, ΔT, should be taken into account as

$$V_0 = V_{\rm sky} + \Delta V, \tag{4}$$

where

$$\Delta V = \frac{V_{\rm sky}}{T_{\rm sky}} \Delta T. \tag{5}$$

We tried to evaluate ΔT from the tipping data in the least-squares fit. However, it was not able to be determined significantly because of a large correlation with other parameters, although we included the data of the large zenith angle (−58° to 58°). This means that ΔT is not very large in the present case. If there would exist the temperature difference of 10 K, the 492 GHz opacity derived assuming $\Delta T = 0$ is systematically underestimated by 10%.

The 220 GHz opacity was evaluated from the output voltages from the receiver at zenith angles of 0°, 48.°2, 60.°0, 66.°4, and 70.°5. Details concerning the observational procedures and analyses of the 220 GHz data were described in Kohno et al. (1995).

5. Discussion

The 492 GHz opacity was compared with the 220 GHz opacity measured simultaneously. The result is shown in figure 3. The time variation of the 492 GHz opacity well corresponds to those of the 220 GHz values both at Pampa la Bola and Rio Frio. The dispersion of the 220 GHz data at Pampa la Bola is much larger than that at Rio Frio, because the performance of the 220 GHz mixer was much better at Rio Frio. In figure 4, we also present the 492 GHz opacity data taken every 2 min in June 30 at Pampa la Bola. The 492 GHz opacity was quite stable during more than 8 hours.

Figure 5 illustrates a correlation diagram between the 492 GHz opacity and the 220 GHz opacity. For this purpose, we picked up 492 GHz and 220 GHz data whose measured times were coincident within 1 min each other. In total, 506 such data points are plotted in figure 5. The data taken at Pampa la Bola and at Rio Frio are indicated by circles and crosses, respectively. The correlation between the 492 GHz and 220 GHz opacities is very good; the correlation coefficient is 0.858 for all of the data. The relation is fitted by the following linear equation:

$$\tau_{492} = a\tau_{220} + b. \tag{6}$$

The coefficients a and b were determined by least-squares analysis to be 20.1 ± 1.5 and 0.057 ± 0.076, respectively, where the errors represent three times the standard deviation. In this calculation the relative weight for each

Table 1. Correlation between τ_{492} and τ_{220}.*

	Altitude (m)	a	b	$r^\dagger$	$\sigma^\S$	$n^\P$
All Data		20.1 ± 1.5	0.057 ± 0.076	0.858	0.294	506
		21.2 ± 0.4	0.000	—	0.295	—
Pampa la Bola	4800	20.6 ± 0.6	0.000	0.871	0.297	305
Rio Frio	4100	21.9 ± 0.6	0.000	0.799	0.276	201

* $\tau_{492} = a\tau_{220} + b$
† Correlation coefficient
§ Standard deviation
¶ Number of data

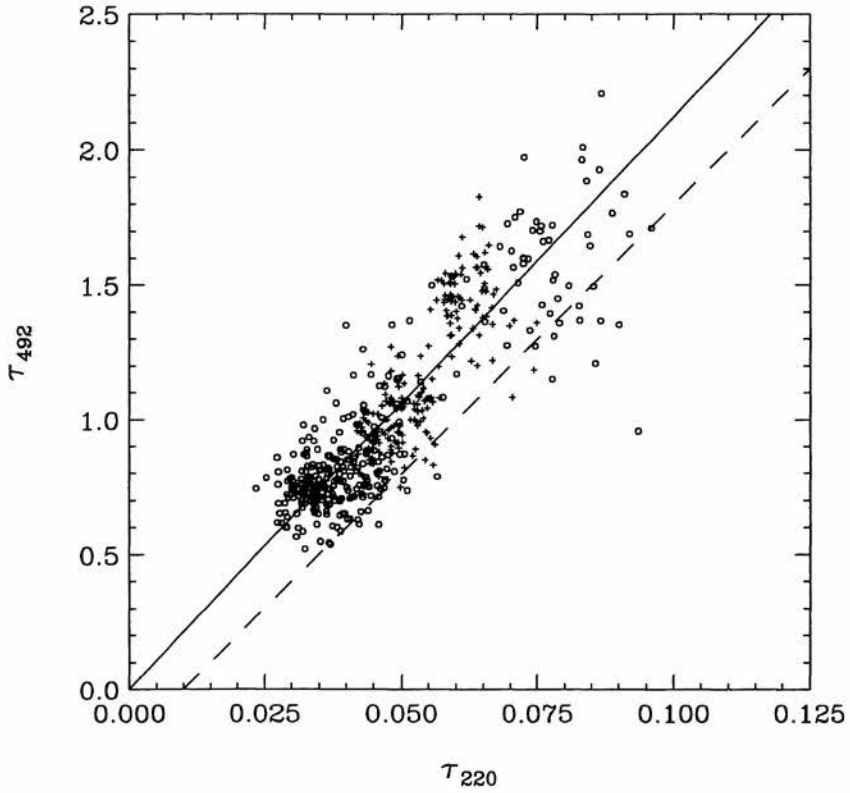

Fig. 5. Correlation diagram between the 492 GHz and 220 GHz opacities. About 500 data taken at Pampa la Bola (circles) and Rio Frio (crosses) are plotted. The solid line represents the best fit; $\tau_{492} = 21.2\ \tau_{220}$. A dashed line represents equation (1); $\tau_{492} = 20(\tau_{225} - 0.01)$, which is observed in Mauna Kea, Hawaii (Masson 1994).

point was taken to be proportional to the inverse square of the standard deviation of the opacity obtained in the least-squares fitting of the tipping data. Since the b constant was not determined significantly, and close to zero, it was fixed to zero. In this case, the a constant represents the ratio of the 492 GHz opacity relative to the 220 GHz opacity, and was determined to be 21.2 ± 0.4. The relationship of equation (1) reported by Masson (1994) is also shown in figure 5.

A similar analysis was carried out for the data taken at Pampa la Bola (figure 6) and those taken at Rio Frio (figure 7) separately. In either case, the b constant was not determined with sufficient accuracy. Hence, we fixed it to zero, and derived only the a constant by a least-squares fit. The results are summarized in table 1. There is no significant difference in the τ_{492}/τ_{220} ratio between the Pampa la Bola and Rio Frio data, although the altitude is different by about 700 m.

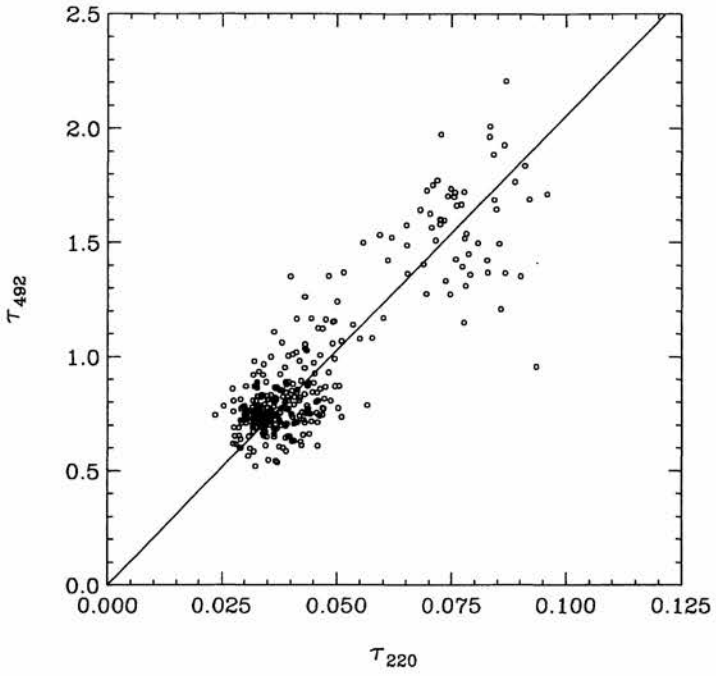

Fig. 6. Correlation diagram between the 492 GHz and 220 GHz opacities measured at Pampa la Bola. The solid line represents the best fit; $\tau_{492} = 20.6\ \tau_{220}$.

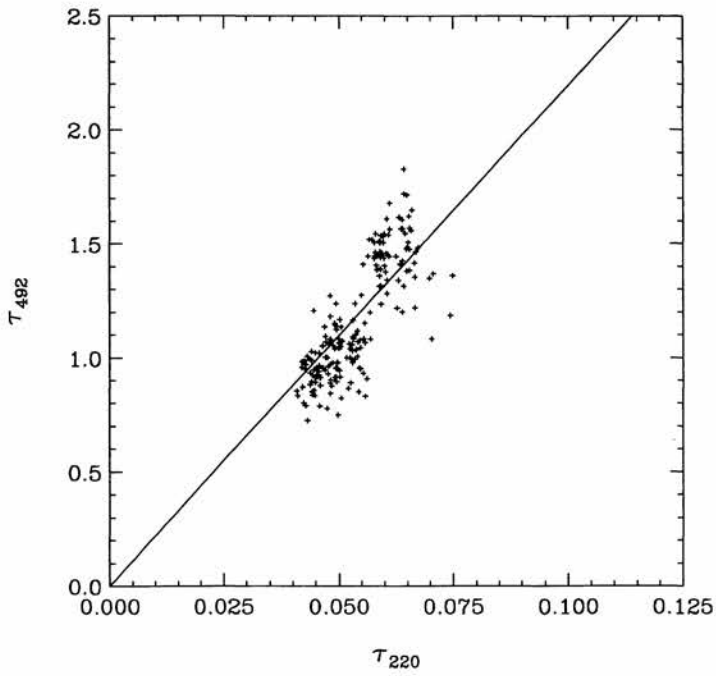

Fig. 7. Correlation diagram between the 492 GHz and 220 GHz opacities measured at Rio Frio. The solid line represents the best fit; $\tau_{492} = 21.9\ \tau_{220}$.

From the present measurements, it has been established that the 492 GHz opacity is proportional to the 220 GHz opacity, and that the ratio is 21.2 ± 0.4 on average in the range of the 492 GHz opacity from 0.5 to 1.5 in northern Chile. Although the observational period was quite short, and was limited in the middle of winter, the present result will provide sound bases for the scaling factor in order to evaluate the 492 GHz opacity from the 220 GHz opacity, which has been almost continuously monitored for more than two years at Rio Frio and Chajnantor.

The dispersion of the τ_{492}/τ_{220} ratio in figure 5 arises mostly from the experimental errors (about 10%). However, it may partly originate from the time variation of the ratio. For example, the 492 GHz opacity seems to increase more steeply than the 220 GHz opacity, as can be seen in the June 28 data (figure 3). Further long-term measurements would be necessary to study such a small variation in detail.

So far, the ratio has been measured to be 20 at Mauna Kea (Masson 1994) and also at the South Pole (elevation 2835 m) (Chamberlin et al. 1997). The present result is almost identical with the values of these two sites. This implies that the standard atmospheric model (Liebe 1989) essentially holds for at least three sites, and that the effect of any local variation from site to site is not very significant. However, we cannot find in our data any offset value as given in equation (1); the b constant in equation (6) was not necessary to interpret our data. This may indicate that the 220 GHz opacity is more free from absorption due to the oxygen molecules than the 225 GHz opacity, as suggested by Chamberlin et al. (1997).

According to the 220 GHz opacity measured at Rio Frio from 1995 July to 1996 February (Holdaway et al. 1996), the fraction of time when the 220 GHz opacity is less than 0.05 is 30% of the total time, although it greatly depends on the years. This means that 30% of the time can be used for submillimeter-wave observations under the condition of the 492 GHz opacity being less than unity. On the other hand, the fraction is 55% for the Chajnantor site from 1995 July to 1996 February (Holdaway et al. 1996). Thus, the two locations at northern Chile can be regarded as being excellent observing sites, and are certainly good candidates for the LMSA project.

Note added in proof (1998 February 13)

Very recently, H. Matsuo and his collaborators of Nobeyama Radio Observatory measured the Fourier transform spectrum of the atmospheric emission in the submillimeter wave region at Pampa la Bola. Their result on the τ_{492}/τ_{220} ratio is almost consistent with ours.

We are grateful to Leonardo Bronfman of University of Chile and Angel Otarola of ESO for helping us in our experiments in northern Chile. This study was supported by the R&D program of Nobeyama Radio Observatory for the LMSA project. TH thanks the Japan Society for the Promotion of Science. SY thanks Sumitomo Foundation and Mitsubishi Foundation for financial support. This study is partly supported by Grant-in-Aids from Ministry of Education, Science, Sports and Culture (07CE2001).

References

Chamberlin R.A., Lane A.P., Stark A.A. 1997, ApJ 476, 428

Holdaway M.A., Ishiguro M., Foster S.M., Kawabe R., Kohno K., Owen F.N., Radford S.J.E., Saito M. 1996, NRO Technical Report, No. 51

Ishiguro M. 1997, in CO: Twenty-Five Years of Millimeter-Wave Spectroscopy, ed W.B. Latter, S.J.E. Radford, P.R. Jewell, J.G. Mangum, J. Bally (Kluwer, Dordrecht) p239

Kohno K., Kawabe R., Ishiguro M., Kato T., Otarola A., Booth R., Bronfman L. 1995, NRO Technical Report, No. 42

Liebe H.J. 1989, Int. J. IR & MM Waves 10, 631

Masson C.R. 1994, in Astronomy with Millimeter and Submillimeter Wave Interferometry, ed M. Ishiguro, W.J. Welch, ASP Conf. Ser. 59, p87

Sekimoto Y., Yoshida H., Hirota T., Takano Y., Furuyama E., Yamamoto S., Saito S., Ozeki H. et al. 1996, Int. J. IR & MM Waves 17, 1263

Yamamoto S., Saito S. 1991, ApJ 370, L103